

# Improved chemical detection using single-walled carbon nanotube network capacitors

J.A. Robinson, E.S. Snow<sup>\*</sup>, F.K. Perkins

*The Naval Research Laboratory, Code 6876, 4555 Overlook Avenue, Washington, DC 20375, United States*

Received 2 May 2006; received in revised form 19 July 2006; accepted 21 July 2006

Available online 7 September 2006

## Abstract

We explore capacitance- and conductance-based detection of trace chemical vapors using single-walled carbon nanotubes (SWNTs). We find that conductance detection is susceptible to such problems as large  $1/f$  noise and incomplete sensor recovery, which are primarily artifacts of a charge-based transduction mechanism. Capacitance detection, dominated by dielectric effects, is less sensitive to charge effects and, thus, offers increased signal-to-noise ratio, improved sensor recovery, and larger dynamic range. Our data indicate capacitance-based sensing with SWNTs is well suited for trace-level detection of such low-vapor-pressure materials as certain chemical warfare agents and explosives. Crown Copyright © 2006 Published by Elsevier B.V. All rights reserved.

**Keywords:** Single-walled carbon nanotube; Chemical detection; Sensor; Capacitance

## 1. Introduction

Single wall carbon nanotubes (SWNT) are a unique nanomaterial consisting entirely of surface atoms [1]. Combining the high surface area of SWNTs with the electronic properties, thermal stability, and chemical inertness of SWNTs means carbon nanotubes are well suited for the chemical detection of trace amounts of chemical vapors. Initial work toward the detection of a vapor phase chemical analyte with a carbon nanotube was based on the measurement of resistance (conductance) variations along a nanotube resulting from tube–analyte interactions [2–7]. Conductance variations are the result of charge transfer between the nanotube and analyte, which alters the number of carriers along the SWNT sidewall [2,3,8]. Proper design of SWNT chemical sensors led to the ability to measure charge transfer as low as 0.1 electrons/SWNT [9].

The high surface-charge sensitivity of the SWNT networks utilized for detection may adversely affect the sensor performance. Charge fluctuations intrinsic to the nanotubes results in increased  $1/f$  noise in conductance measurements [10], and the presence of water induces hysteresis in the drain current versus gate voltage in SWNT-channel field effect transistors [11].

Charge transfer from adsorbed molecules bound to metastable sites along the SWNT may also lead to incomplete sensor recovery of measured conductance to pre-exposure levels [3,6].

Capacitance-based detection provides superior sensitivity and recovery compared to conductance-based detection for most chemical vapors. We recently reported the use of a capacitance-response device (chemicapacitor) that combines stability, high sensitivity and fast response time to a large variety of analytes [12]. In this sensor, a SWNT network, SiO<sub>2</sub> insulating layer, and Si substrate form a parallel plate capacitor. When a voltage is applied between the network and the degenerately doped substrate a large electric field gradient is formed around the SWNTs. The electric field radiating from the SWNT creates a new polarization of the adsorbates (relative to the unbiased state), which is measured as a change in the capacitance of the system. For most chemical vapors, this method of chemical detection exhibits fewer charge-dependent artifacts than SWNT chemiresistor measurements [13].

In the following pages, we report new capacitance and conductance data from SWNT networks in the presence of chemical vapors. Charge dependence, device recovery, and chemical sensitivity of chemicapacitor measurements will be addressed for a variety of analytes. The capacitance response produces a higher signal-to-noise ratio, exhibits improved sensor recovery, and has a larger dynamic range than SWNT conductance measurements. The response to analyte concentration is sub-linear for most

<sup>\*</sup> Corresponding author. Fax: +1 202 767 1165.

E-mail address: [snow@bloch.nrl.navy.mil](mailto:snow@bloch.nrl.navy.mil) (E.S. Snow).

Report Documentation Page			Form Approved OMB No. 0704-0188		
Public reporting burden for the collection of information is estimated to average 1 hour per response, including the time for reviewing instructions, searching existing data sources, gathering and maintaining the data needed, and completing and reviewing the collection of information. Send comments regarding this burden estimate or any other aspect of this collection of information, including suggestions for reducing this burden, to Washington Headquarters Services, Directorate for Information Operations and Reports, 1215 Jefferson Davis Highway, Suite 1204, Arlington VA 22202-4302. Respondents should be aware that notwithstanding any other provision of law, no person shall be subject to a penalty for failing to comply with a collection of information if it does not display a currently valid OMB control number.					
1. REPORT DATE <b>JUL 2006</b>		2. REPORT TYPE		3. DATES COVERED <b>00-00-2006 to 00-00-2006</b>	
4. TITLE AND SUBTITLE <b>Improved chemical detection using single-walled carbon nanotube network capacitors</b>			5a. CONTRACT NUMBER		
			5b. GRANT NUMBER		
			5c. PROGRAM ELEMENT NUMBER		
6. AUTHOR(S)			5d. PROJECT NUMBER		
			5e. TASK NUMBER		
			5f. WORK UNIT NUMBER		
7. PERFORMING ORGANIZATION NAME(S) AND ADDRESS(ES) <b>Naval Research Laboratory, Code 6876, 4555 Overlook Avenue SW, Washington, DC, 20375</b>			8. PERFORMING ORGANIZATION REPORT NUMBER		
9. SPONSORING/MONITORING AGENCY NAME(S) AND ADDRESS(ES)			10. SPONSOR/MONITOR'S ACRONYM(S)		
			11. SPONSOR/MONITOR'S REPORT NUMBER(S)		
12. DISTRIBUTION/AVAILABILITY STATEMENT <b>Approved for public release; distribution unlimited</b>					
13. SUPPLEMENTARY NOTES					
14. ABSTRACT <b>We explore capacitance- and conductance-based detection of trace chemical vapors using single-walled carbon nanotubes (SWNTs). We find that conductance detection is susceptible to such problems as large 1/f noise and incomplete sensor recovery, which are primarily artifacts of a charge-based transduction mechanism. Capacitance detection, dominated by dielectric effects, is less sensitive to charge effects and, thus, offers increased signal-to-noise ratio, improved sensor recovery, and larger dynamic range. Our data indicate capacitance-based sensing with SWNTs is well suited for trace-level detection of such low-vapor-pressure materials as certain chemical warfare agents and explosives.</b>					
15. SUBJECT TERMS					
16. SECURITY CLASSIFICATION OF:			17. LIMITATION OF ABSTRACT <b>Same as Report (SAR)</b>	18. NUMBER OF PAGES <b>6</b>	19a. NAME OF RESPONSIBLE PERSON
a. REPORT <b>unclassified</b>	b. ABSTRACT <b>unclassified</b>	c. THIS PAGE <b>unclassified</b>			

analytes and is a function of the partial pressure of the analyte ( $P/P_0$ ), not the equilibrium vapor pressure ( $P_0$ ). This is particularly advantageous for low-vapor-pressure materials, such as chemical nerve agents and explosives, and suggests minimal detection levels (MDL) below 1 ppb.

## 2. Experimental procedure

The SWNT sensors were fabricated on a 1200 Å thick SiO<sub>2</sub> thermal oxide, which was grown on a degenerately doped n-type Si substrate. Chemical vapor deposition of the SWNTs was accomplished at 800 °C using an iron nitrate catalyst under flowing argon, hydrogen, and ethylene. Each sensor consists of a 2 mm × 2 mm interdigitated array of two Ti/Au (100/1000 Å) contacts evaporated onto the SWNT network, with associated pads for probing. The interdigitation gives a channel length and width of 0.34 and 10 mm, respectively [13]. Contacts were fabricated using standard ultraviolet lithography techniques. Following metal deposition, excess metal was lifted off, and the device channel array was coated with photoresist prior to a two minute oxygen plasma etch. The purpose of the oxygen plasma etch is to isolate adjacent devices from one another. Following the etch, the resist was stripped using acetone and the device chips were soaked in Baker PRS1000 (Mallinkrodt Baker Inc., Phillipsburg, NJ; <http://www.jtbaker.com>) held at a temperature of 80 °C to ensure the devices were clear of any organic contaminants prior to use in the laboratory.

The conductance through the network is measured using a Stanford Research Systems model SR830 DSP lock-in amplifier, observing a voltage  $V_G$  generated by an applied ac bias voltage ( $V_{G0}$ ) of 100 mV<sub>rms</sub> at a frequency of 150 Hz. A lock-in amplifier is also used to measure the capacitance of the sensor, by observing a signal  $V_C$  generated by an ac voltage ( $V_{C0}$ ) at  $f = 5$  kHz and amplitude 200 mV peak-to-peak from an Agilent 33250A Signal Generator connected to the substrate. For simultaneous measurements of conductance and capacitance, a polypropylene capacitor is connected between the two electrodes and a metal film resistor between one electrode and voltage source for conductance measurements [13]. The capacitor value, typically 10 μF, is chosen so as to appear as an open circuit element at the frequency of the conductance signal and a short circuit at the capacitance frequency. The resistor value ( $R_L$ ) is set to exceed the SWNT network impedance and thus minimize capacitance signal losses through the low impedance of the conductance signal source. The other electrode is connected to both lock-in amplifier inputs with a 1 kΩ resistor ( $R_B$ ) from that point to ground as a simple current–voltage converter. In these voltage divider circuits, the capacitance  $C$  is then found from  $C = [2\pi f R_B (V_{C0}/V_C - 1)]^{-1}$  and the conductance  $G$  from  $G = [R_B (V_{G0}/V_G - 1) - R_L]^{-1}$ . Using this device setup we are capable of measuring normalized conductance response ( $\Delta G/G$ ) and capacitance response ( $\Delta C/C$ ) values as small as 0.0001 [13].

In order to establish the MDL of the various analytes, the noise level for capacitance and conductance measurements must be known. For capacitance noise, the two electrodes are connected directly to the voltage input of the lock-in amplifier with

a parallel 1 kΩ wire-wound resistor to ground. The sensor gate is connected to the internal ac source on the lock-in amplifier. For conductance noise, the lock-in amplifier internal source is connected to one electrode, the other electrode is connected to one of the voltage inputs to the lock-in amplifier along with a 1 kΩ wire-wound resistor to circuit common. The source amplitude for both measurements,  $V_{G0}$  and  $V_{C0}$ , is adjusted so as to generate a 10 mV<sub>rms</sub> signal at the lock-in input. The amplified, filtered output from the lock-in amplifier is fed into a Hewlett Packard 3582A Spectrum Analyzer. A Hanning window is applied to the sampled data, which is subsequently transformed into frequency space and averaged for a sufficient period to generate a relatively smooth power spectrum. A detailed description of the experimental procedure for 1/ $f$  noise measurements is explained in a subsequent publication [14].

For all response characterization, a flow across the device under test of 5 lpm of dry air is maintained. Chemical vapors were delivered to the devices via a bubbler system capable of analyte concentrations ranging from 0.0002 to 0.5 of the equilibrium pressure ( $P_0$ ). Delivery of the chemicals was accomplished by mixing saturated vapors of the chemical analyte with dry air at varying ratios to achieve the desired dilution ( $P/P_0$ ). Low-vapor-pressure analytes, such as 2,4-dinitrotoluene (DNT), required longer mixing times to reach equilibrium; however, the majority of analytes tested reached equilibrium (peak  $\Delta G/G$  and  $\Delta C/C$  response of our sensors) within a few seconds. The measured response time is a characteristic of the vapor delivery system, not of the sensors themselves.

## 3. Results and discussion

Basic knowledge of the chemiresistor and chemicapacitor responses to various analytes is an important step in understanding how these devices will perform. The conductance ( $G$ ) of SWNTs is proportional to the number ( $n_h$ ) and mobility ( $\mu_h$ ) of charge carriers at the surface of the nanotube ( $G = qn_h\mu_h$ ). As a result, the conductance will be heavily influenced by charge transfer from an adsorbate and variations in carrier mobility in the nanotube.

The total SWNT network capacitance may be modeled as two capacitors in series,  $C = (1/C_g + 1/C_Q)^{-1}$  where  $C_g$  is the gate capacitance, which includes the oxide dielectric and dielectric effects of the adsorbates, and  $C_Q$  is the quantum (charge-based) capacitance, which is a function of the Fermi energy in the SWNTs [15]. Adsorbate charge transfer can shift the Fermi level into a region with a different density of states, resulting in a change in  $C_Q$ . In the case where the energy of the carrier is much greater than  $E_g/2$ , where  $E_g$  is the SWNT band gap, the quantum capacitance is approximately one order of magnitude greater than the gate capacitance [15]. As a result, the total capacitance is dominated by the gate capacitance with a small contribution from quantum capacitance, leading to a weak charge dependence.

The capacitance response ( $\Delta C$ ) to an analyte is caused by field-induced polarization of surface dipoles, and contains contributions from both the dielectric ( $\epsilon$ ) and the charge ( $Q$ ) effects of the analyte [13]. This response can be modeled as

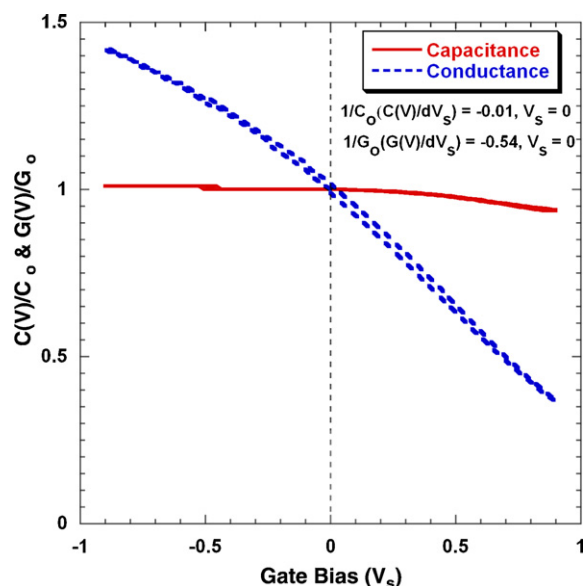


Fig. 1. Normalized current–voltage and capacitance–voltage measurements of a typical SWNT chemical sensor.

$\Delta C = \delta C / \delta \varepsilon \Delta \varepsilon + \delta C / \delta Q \Delta Q$ , where the dielectric effect from the adsorbed analyte is described as  $\delta C / \delta \varepsilon \Delta \varepsilon$ , and the charge dependence as a result of the quantum capacitance is  $\delta C / \delta Q \Delta Q$ . Measurements to quantitatively determine the relative contributions of the charge and dielectric response indicate the charge-based response is less than 10% of the total  $\Delta C$  [13].

To illustrate the dependence of conductance and capacitance on charge, it is instructive to discuss current–voltage and capacitance–voltage characteristics of the SWNT sensors. To do this, conductance ( $G$ ) and capacitance ( $C$ ) were monitored as a function of substrate bias ( $V_s$ ). Fig. 1 is a plot of the normalized differential capacitance ( $C(V_s)/C_0$ ) and conductance ( $G(V_s)/G_0$ ) response, where  $C_0$  and  $G_0$  are the zero bias capacitance and conductance, respectively. Using  $Q = CV_s$ , the slope of each curve at  $V_s = 0$  is an indication of the capacitance and conductance charge sensitivity of our sensors. As is evident from Fig. 1, the slope of  $1/G_0(G(V_s)/dV_s)$  is greater than  $1/C_0(C(V_s)/dV_s)$ . The calculated slope of the normalized conductance and capacitance is  $-0.54$  and  $-0.01 \text{ V}^{-1}$ , respectively. Accordingly, it is expected that a fixed amount of charge transfer will yield a conductance response over an order of magnitude greater than the capacitance response. It should be noted that  $1/G_0(G(V_s)/dV_s)$  is typically 10–60 times  $1/C_0(C(V_s)/dV_s)$ .

Charge sensitivity accounts for the relative conductance and capacitance sensitivity to the random charge fluctuations in SWNTs that give rise to  $1/f$  noise. It has been shown that conductance is much more dependent on charge fluctuations; as a result, the charge dependence could result in larger  $1/f$  noise characteristics compared to  $1/f$  noise found in capacitance measurements. Fig. 2 is a typical  $1/f$  noise spectrum for a SWNT network device. Clearly, the capacitance noise spectral density ( $\text{V}^2/\text{Hz}$ ) is substantially quieter, by a factor of 2000, than conductance noise. Indeed, the observed capacitance spectral noise density above 10 Hz appears to be limited by the lock-in preamplifier input Johnson noise density of  $2.5 \times 10^{-16} \text{ V}^2/\text{Hz}$ . At lower fre-

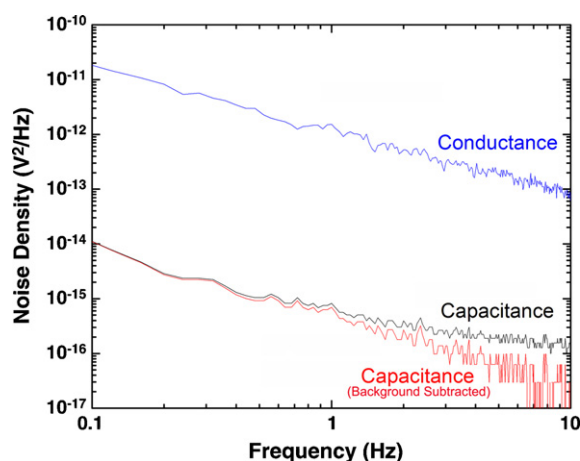


Fig. 2. Comparison of low-frequency noise of conductance and capacitance of a SWNT network sensor.

quencies, both capacitance and conductance measurements are dominated by  $1/f$  noise. Carbon nanotube devices are well known to generate significant  $1/f$  noise [10]. This is clearly a significant fraction of the conductance signal measurements. However, by integrating the data in Fig. 2 over an assumed a measurement bandwidth from 0.1 to 10 Hz, we find the mean square amplitude for capacitance noise ( $V_{\text{cn}}^2$ ) to be  $2.6 \times 10^{-15} \text{ V}^2$ . Defining a minimum detectable signal as three times the rms noise amplitude gives  $V_{\text{Cmin}} = 1 \times 10^{-7}$ . Given that the input to the lock-in amplifier  $V_C$  is set to be 10 mV, this suggests a measurable  $\Delta C/C$  as low as  $10^{-5}$ . However, it should be noted that this configuration is optimized to measure the SWNT network limiting noise level. The noise of a more practical system limits the minimum  $\Delta C/C$  to a somewhat higher level of  $10^{-4}$ .

The charge sensitivity of SWNTs allow one to observe very dilute amounts of certain adsorbates in the ambient environment; however, it also leads to irregular response behavior and sensor non-recoverability. The conductance response of a SWNT network sensor to doses of toluene illustrates some of the irregular behavior and non-recoverability associated with charge dependence. Fig. 3 illustrates the normalized capacitance and conductance responses to five-second doses of toluene ranging from 0.1 to 8%  $P/P_0$  (40–3000 ppm). At low concentrations ( $<1\% P/P_0$ ), the conduction of the SWNT network responds to the analyte slowly, does not recover when the source of analyte is turned off, and decreases as  $P/P_0$  increases. However, as the concentration of the analyte is increased, the conduction response reverses sign and begins to increase with dose, and corresponds better with applied dose. This non-linear behavior indicates there may be competing mechanisms contributing to the SWNT conduction, or perhaps different nanotube–analyte interactions based on the individual nanotube properties. One possible mechanism for the conductance response includes different types of binding sites on the nanotubes resulting in varying responses. When the lower energy sites are saturated, the next level of sites dominates the response, which would account for the change in nature of the conductance response to toluene partial pressure.

While chemiresistors generally yield predictable conductance responses when initially exposed to the majority of ana-

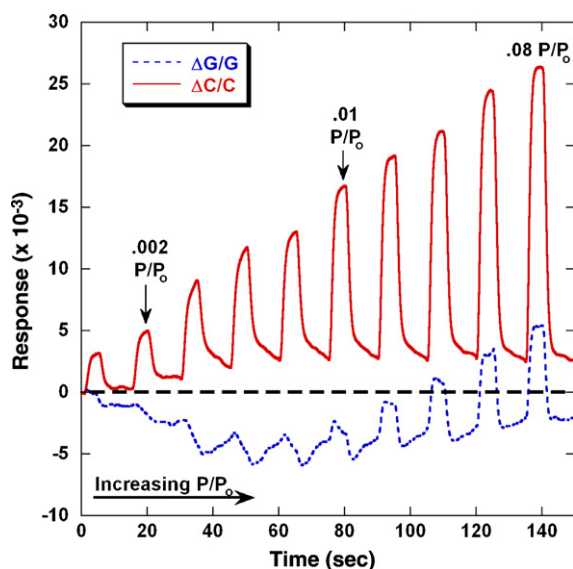


Fig. 3. Normalized capacitance and conductance response as a function of toluene concentration. The capacitance recovers to within 10%  $\Delta C/C$  of the baseline while conductance is unpredictable.

lytes, we frequently observe a failure of the sensor to fully recover following exposure to certain analytes. SWNT defects result in low energy binding sites along the nanotube; [16] as a result, a small portion of the molecules that adsorb to the nanotubes will remain on the nanotube surface in a metastable state. The conduction properties of the SWNT will thus be altered on a more permanent basis, leading to a “new” baseline conductance. Researchers found that either heating the device, by using a voltage spike, or dosing the device with ultraviolet light after exposure is required to bring the conduction signal back to its original baseline [3,7,17]. Device capacitance is less sensitive to charge, and as a result the measured capacitance will be less subject to irregular behavior.

The capacitance response of a SWNT network sensor is dominated by the dielectric effect of an adsorbate and is not affected as severely by metastable binding sites. The capacitance response to toluene in Fig. 3 exhibits predictable and reproducible values that monotonically increase with toluene concentration. There is a non-recoverable portion of the capacitance response (a slight drift from the original baseline). We attribute this to the effect of a net charge transfer on the quantum capacitance [13]. In contrast, the conductance response is difficult to predict as a function of toluene  $P/P_0$ . Evident from Fig. 3, various molecule/nanotube interactions contribute competing charge polarities, yielding a conductance response that decreases initially but eventually increases as a function of  $P/P_0$ . The conductance response also varies between devices, indicating that for toluene, the conductance along the nanotube network is heavily dependent on the type of active sites available for charge transfer. The exact origin of the charge transfer is not fully understood.

A practical sensor must be capable of operation over a large range of analyte concentrations. However, the conductance response can saturate even at moderate analyte concentrations. To illustrate this effect, 5 s doses of acetone ranging from 0.0002  $P/P_0$  to 0.5  $P/P_0$  were used to allow measurement of capaci-

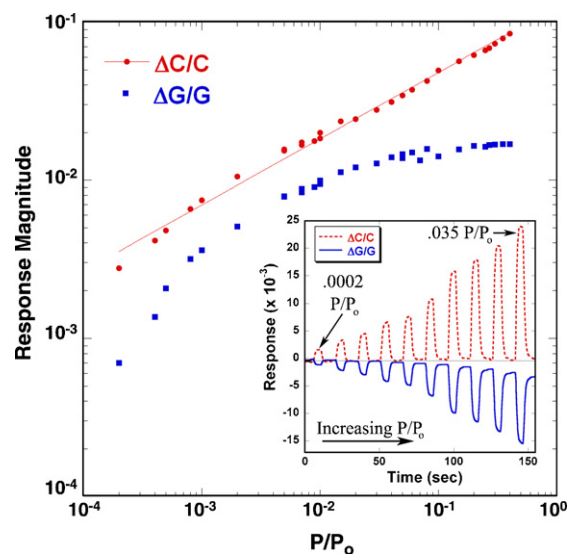


Fig. 4. Capacitance and conductance response to sequential doses of acetone ranging from 0.0001 to 0.5  $P/P_0$ . The conductance response saturates at  $\sim 0.05 P/P_0$ .

tance and conductance response over three orders of magnitude of concentration. As illustrated in Fig. 4, the magnitude of the conductance response ( $\Delta G/G$ ) saturates at  $P/P_0 \sim 0.05$ , indicating that the sites responsible for the variation in conductance are fully occupied by the analyte at 0.05  $P/P_0$ . It is useful to note, however, that the conductance response varies proportionally to the amount of charge transfer from the analyte. Analytes that bind more tightly with the SWNTs and exhibit larger charge transfer are expected to affect the carrier density and mobility to a greater extent than those that only weakly physisorb [8].

The capacitance response ( $\Delta C/C$ ) is a measure of the polarization of condensed material (e.g., adsorbates) and is not subject to response saturation. As analyte collects on the SWNTs, the electric field intersects an increasing number of analyte molecules beyond those molecules that bind to the active sites on the nanotube sidewall, resulting in a capacitance response that is essentially linear over the full range of analyte concentrations. As a result, a capacitive-response device will exhibit dynamic ranges greater than a measurement that relies strongly on charge transfer. Also evident from Fig. 4 (and Fig. 3) is the relative sensitivity of the capacitance and conductance. Over the non-saturated response, it is clear the capacitance response is more sensitive to the presence of analyte than its conductance counterpart.

In general the capacitive response to an analyte is more sensitive than the conduction response, and it increases monotonically with analyte concentration without saturating. Fig. 5 illustrates the normalized capacitance response ( $\Delta C/C$ ) as a function of  $P/P_0$  for various analytes. As is evident from the data, all tested analytes follow a simple power law relationship:  $\Delta C/C = \alpha(P/P_0)^n$ , with  $0.01 < \alpha < 0.15$  and  $0.4 < n < 1$ . Also evident is that both high-vapor-pressure analytes, such as acetone, and low-vapor-pressure analytes, such as 2,4-dinitrotoluene (DNT), can produce comparable responses at a fixed value of  $P/P_0$ .



Table 1  
Predicted minimal detection limits (MDL) of various analytes

Analyte	Power law fit ( $\Delta C/C = \alpha(P/P_0)^n$ )		Extrapolated detection limits		
	$\alpha$	$n$	MDL ( $P/P_0$ )	$P_0$ at 25 °C (mbar)	MDL (ppb)
DMMP	0.11	0.38	$9.9 \times 10^{-9}$	1.6	0.016
DNT	0.11	0.57	$4.6 \times 10^{-6}$	0.00028	0.0013
Acetone	0.14	0.53	$1.2 \times 10^{-6}$	304	352
Toluene	0.08	0.45	$3.5 \times 10^{-7}$	31	11
Methanol	0.15	0.87	$2.2 \times 10^{-4}$	168	$3.75 \times 10^4$
Water	0.02	0.82	$1.5 \times 10^{-3}$	32	$5.0 \times 10^4$
Hexane	0.02	0.78	$1.1 \times 10^{-3}$	200	$2.24 \times 10^5$
Chlorobenzene	0.07	0.92	$8.1 \times 10^{-4}$	16	$1.29 \times 10^4$

Also shown in Fig. 5 is our conservative minimal detection limit (MDL) of  $\Delta C/C = 10^{-4}$ . Using our current vapor delivery system, analytes with high-vapor pressures have a minimum measurable  $P/P_0$  of 0.0002. For low-vapor-pressure analytes (particularly DNT) the minimum  $P/P_0$  was several orders of magnitude higher at 0.01. The sensitivity for a particular molecule is determined by the interaction with the SWNTs, the intrinsic molecular dipole moment, and preferred orientation of the dipole on the SWNT surface. Extrapolation of the sub-linear response observed in our data to the minimum detectable  $\Delta C/C$  implies ultra low detection limits and large dynamic ranges.

The capacitance response to dimethylmethylphosphonate (DMMP) and DNT is highly sub-linear with exponent values of  $\sim 0.4$  and  $\sim 0.6$ , respectively, indicating MDLs below the ppb range may be obtainable. Table 1 presents a best fit of the data represented in Fig. 5. To the best of our knowledge, the lowest reported MDL for DMMP is 20 ppb with a response time of 10 s [18]. Direct measurement of 800 ppb DMMP ( $P/P_0 = 0.0005$ ) with  $\Delta C/C = 0.006$  and a recovery time of 2 s was accomplished in this study. This value is 60 times larger than our estimated  $\Delta C/C$  detection limit, indicating that if DMMP continues to follow the power law relationship in Fig. 5, a MDL for DMMP of 0.02 ppb is expected. Similar results for DNT were also

recorded. Using the current vapor delivery system, direct detection of 5.6 ppb DNT ( $0.02 P/P_0$ ) was accomplished with a  $\Delta C/C$  value of 0.007. Extrapolation of the curve presented in Fig. 5 yields a MDL of approximately 0.001 ppb. The current published MDL for DNT is 0.3 ppb [19]. It should be noted, however, that verification of the predicted MDLs of all analytes is pending. It is quite possible that the response of the chemicapacitor may become linear in the region below the minimum testable  $P/P_0$  values, resulting in higher MDLs than calculated in Table 1.

#### 4. Conclusions

Chemical detection using single wall carbon nanotubes has been discussed. We find that conductance detection is susceptible to large  $1/f$  noise, incomplete sensor recovery, and limited dynamic range, which are primarily artifacts of a charge-based transduction mechanism. The use of a dielectric effect and polarization transduction mechanism is more sensitive and reliable for chemical detection. The capacitive response to adsorbates exhibits a monotonic increase with  $P/P_0$  over a large dynamic range without saturation effects. Finally, the response is a sub-linear function of the partial pressure of most analytes, indicating the detection of low-vapor-pressure materials, such as DMMP and DNT, may be possible well into the parts-per-trillion range.

#### Acknowledgements

Financial support for J.A. Robinson is provided through the National Academy of Sciences, National Research Council.

#### References

- [1] M.S. Dresselhaus, G. Dresselhaus, A. Jorio, Unusual properties and structure of carbon nanotubes, *Annu. Rev. Mater. Res.* 34 (2004) 247–278.
- [2] J. Kong, N. Franklin, C. Zhou, M. Chapline, S. Peng, K. Cho, H. Dai, Nanotube molecular wires as chemical sensors, *Science* 287 (2000) 622–625.
- [3] J.P. Novak, E.S. Snow, E.H. Houser, D. Park, J.L. Stepnowski, R.A. McGill, Nerve agent detection using networks of single-walled carbon nanotubes, *Appl. Phys. Lett.* 83 (2003) 4026–4028.
- [4] E. Bekyarova, M. Davis, T. Burch, M.E. Itkis, B. Zhao, S. Sunshine, R.C. Haddon, Chemically functionalized single-walled carbon nanotubes as ammonia sensors, *J. Phys. Chem. B* 108 (2004) 19717–19720.
- [5] P. Collins, K. Bradley, M. Ishigami, A. Zettl, Extreme oxygen sensitivity of electronic properties of carbon nanotubes, *Science* 287 (2000) 1801–1804.
- [6] P. Qi, O. Vermesh, M. Grecu, A. Javey, Q. Wang, H. Dai, S. Peng, K. Cho, Toward large arrays of multiplex functionalized carbon nanotube sensors

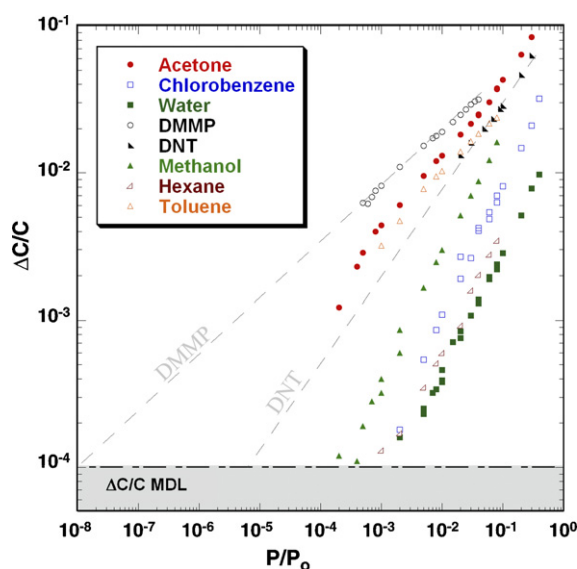


Fig. 5. Capacitive response ( $\Delta C/C$ ) to various analytes as a function of  $P/P_0$ .

- for highly sensitive and selective molecular detection, *Nanoletter* 3 (2003) 347–351.
- [7] J. Li, Y. Lu, Q. Ye, M. Cinke, J. Han, M. Meyyappan, Carbon nanotube sensors for gas and organic vapor detection, *Nanoletter* 3 (2003) 929–933.
- [8] J. Zhao, A. Buldum, J. Han, J. Lu, Gas molecule adsorption in carbon nanotubes and nanotube bundles, *Nanotechnology* 13 (2002) 195–200.
- [9] E.S. Snow, F.K. Perkins, J.A. Robinson, Chemical detection using single-walled carbon nanotubes, *Chem. Soc. Rev.* 35 (2006) 790–798.
- [10] E.S. Snow, J.P. Novak, M.D. Lay, F.K. Perkins,  $1/f$  noise in single-walled carbon nanotube devices, *Appl. Phys. Lett.* 85 (2004) 4172–4174.
- [11] W. Kim, A. Javey, O. Vermesh, Q. Wang, Y. Li, H. Dai, Hysteresis caused by water molecules in carbon nanotube field-effect transistors, *Nanoletter* 3 (2003) 193–198.
- [12] E.S. Snow, F.K. Perkins, E.H. Houser, S.C. Badescu, T.L. Reinecke, Chemical detection with a single-walled carbon nanotube capacitor, *Science* 307 (2005) 1942–1945.
- [13] E.S. Snow, F.K. Perkins, Capacitance and conductance of single-walled carbon nanotubes in the presence of chemical vapors, *Nanoletter* 5 (2005) 2414–2417.
- [14] F.K. Perkins, E.S. Snow, in preparation.
- [15] S. Rosenblatt, Y. Yaish, J. Park, J. Gore, V. Sazonova, P. McEuen, High performance electrolyte gated carbon nanotube transistors, *Nanoletter* 2 (2002) 869–872.
- [16] M. Grujici, G. Cao, R. Singh, The effect of topological defects and oxygen adsorption on the electronic transport properties of single-walled carbon-nanotubes, *Appl. Surf. Sci.* 211 (2003) 166–183.
- [17] W. Wongwriyapan, S. Honda, H. Konishi, T. Mizuta, T. Ikuno, T. Ito, T. Maekawa, K. Suzuki, H. Ishikawa, K. Oura, M. Katayama, Single-walled carbon nanotube thin-film sensor for ultrasensitive gas detection, *Jpn. J. Appl. Phys.* 44 (2005) L482–L484.
- [18] I. Voiculescu, M. Zaghloul, R. McGill, E. Houser, G. Fedder, Electrostatically actuated resonant microcantilever beam in CMOS technology for the detection of chemical weapons, *IEEE Sens.* 5 (2005) 641.
- [19] L.A. Pinnaduwa, T. Thundat, J.E. Hawk, D.L. Heddena, P.F. Britt, E.J. Houser, S. Stepnowski, R.A. McGill, D. Bubb, Detection of 2,4-dinitrotoluene using microcantilever sensors, *Sens. Actuators B* 99 (2004) 223–229.